some loss of D^0 because of ionization is also possible. By using these results, we can extract the quantum process tomography (*25*) of the sequence, confirming the close resemblance to the identity operator.

The AEDMR mechanism we introduce here should be extensible to the readout of single ^{31}P impurities (*17*, *30*) and could be combined with the already demonstrated spin-dependent–tunneling electron spin readout of single ^{31}P (*14*). The method can be applied to other substitutional donors when ^{28}Si samples become available, and in particular Bi, where the much larger hyperfine coupling makes the hyperfine D^0X structure almost resolvable even in natural Si (*20*). The present p-type sample, together with our optical methods, would also be suited well to explore the NMR of ionized ^{31}P (D^+), which has recently been observed by using electrically detected ENDOR in natural Si (*13*) and should have very long T_{2n} in ^{28}Si. Such results would be important for the proposed cluster-state quantum computing scheme where quantum information is stored in the nuclear spins of ionized donors (*31*).

By eliminating almost all inhomogeneous broadening and host spins, highly enriched ^{28}Si approaches a semiconductor vacuum, enabling the use of hyperfine-resolved optical transitions, as is standard for atom and ion qubits in vacuum, but retaining the advantages of Si device technology, Auger photoionization for polarization and readout, and the ability to precisely and permanently place the qubit atoms (*32*).

References and Notes

1. D. Deutsch, *Proc. R. Soc. London Ser. A* **400**, 97 (1985).
2. J. P. Home *et al.*, *Science* **325**, 1227 (2009); 10.1126/science.1177077.
3. J. J. L. Morton, D. R. McCamey, M. A. Eriksson, S. A. Lyon, *Nature* **479**, 345 (2011).
4. P. Becker, H.-J. Pohl, H. Riemann, N. V. Abrosimov, *Phys. Status Solidi A* **207**, 49 (2010).
5. T. D. Ladd *et al.*, *Nature* **464**, 45 (2010).
6. B. E. Kane, *Nature* **393**, 133 (1998).
7. J. J. L. Morton *et al.*, *Nature* **455**, 1085 (2008).
8. D. R. McCamey, J. Van Tol, G. W. Morley, C. Boehme, *Science* **330**, 1652 (2010).
9. S. Simmons *et al.*, *Nature* **470**, 69 (2011).
10. A. M. Tyryshkin *et al.*, *Nat. Mater.* **11**, 143 (2012).
11. D. R. McCamey, J. van Tol, G. W. Morley, C. Boehme, *Phys. Rev. Lett.* **102**, 027601 (2009).
12. H. Morishita *et al.*, *Phys. Rev. B* **80**, 205206 (2009).
13. L. Dreher, F. Hoehne, M. Stutzmann, M. S. Brandt, *Phys. Rev. Lett.* **108**, 027602 (2012).
14. A. Morello *et al.*, *Nature* **467**, 687 (2010).
15. W. M. Witzel, M. S. Carroll, A. Morello, Ł. Cywiński, S. Das Sarma, *Phys. Rev. Lett.* **105**, 187602 (2010).
16. M. Cardona, M. L. W. Thewalt, *Rev. Mod. Phys.* **77**, 1173 (2005).
17. A. Yang *et al.*, *Phys. Rev. Lett.* **97**, 227401 (2006).
18. A. Yang *et al.*, *Phys. Rev. Lett.* **102**, 257401 (2009).
19. M. Steger *et al.*, *J. Appl. Phys.* **109**, 102411 (2011).
20. T. Sekiguchi *et al.*, *Phys. Rev. Lett.* **104**, 137 (2010).
21. T. D. Ladd, D. Maryenko, Y. Yamamoto, E. Abe, K *Phys. Rev. B* **71**, 014401 (2005).
22. C. Langer *et al.*, *Phys. Rev. Lett.* **95**, 060502 (2
23. A. Yang *et al.*, *Appl. Phys. Lett.* **95**, 122113 (2
24. W. Schmid, *Phys. Status Solidi B* **84**, 529 (197
25. Materials and methods are available as supplen materials on *Science* Online.
26. L. Viola, S. Lloyd, *Phys. Rev. A* **58**, 2733 (1998
27. A. M. Tyryshkin *et al.*, http://arxiv.org/abs/:1011 (2010).
28. T. Gullion, D. B. Baker, M. S. Conradi, *J. Magn.* **89**, 479 (1990).
29. G. Feher, E. A. Gere, *Phys. Rev.* **114**, 1245 (19
30. D. Sleiter *et al.*, *New J. Phys.* **12**, 093028 (201
31. J. J. L. Morton, http://arxiv.org/abs/0905.400 (2009).
32. S. R. Schofield *et al.*, *Phys. Rev. Lett.* **91**, 13610

Acknowledgments: This work was supported by the Natural Sciences and Engineering Research Council o Canada (NSERC). J.J.L.M. acknowledges support from Royal Society (UK), St. John's College, Oxford, the En and Physical Sciences Research Council (EP/I035536/ and a European Research Council Starter Grant.

Supplementary Materials

www.sciencemag.org/cgi/content/full/336/6086/1280/
Materials and Methods
Supplementary Text
Figs. S1 and S2
References (*33*–*37*)

8 December 2011; accepted 13 April 2012
10.1126/science.1217635

Room-Temperature Quantum Bit

combination of laser illumination and

frequency (rf) decoupling pulse sequences

The spin transition between the $|0\rangle \rightarrow |-1\rangle$ electronic spin states was addressed via microwave radiation (*15*). Figure 1B shows the free-electron precession of an individual NV center, measured via a Ramsey sequence. The signal dephased on a time scale of $T_{2e}^{*} = 470 \pm 100$ μs, which is consistent with the given isotopic purity of the sample (*14*). The characteristic collapses and revivals of the Ramsey signal correspond to the signature of a single weakly coupled ^{13}C nuclear spin. This coupling strength, originating from a hyperfine interaction, corresponds to an electron-nuclear separation of roughly 1.7 nm (*15*).

To confirm that the signal originated from a ^{13}C nuclear spin, we measured the probability of a rf-induced nuclear spin-flip as a function of carrier frequency, ω. As described below, we prepared the nuclear spin in either the $|\downarrow\rangle$ or $|\uparrow\rangle$ state by performing a projective measurement. After preparation of the nuclear spin via projection, a 1.25-ms Gaussian shaped rf π-pulse was applied. A second step of nuclear measurement then allowed the nuclear spin-flip to be determined. Figure 1C shows that this probability is characterized by three resonances located at $\omega/(2\pi) = 258.86$, 261.52, and 264.18 kHz, corresponding to the NV electronic spin being in $m_s = 1,0,-1$, respectively; this indicates a projected hyperfine interaction $A_{\parallel} = (2\pi)\ (2.66 \pm 0.08)$ kHz.

An important facet of quantum control involves the ability to perform high-fidelity initialization and readout. We used repetitive readout to nuclear spin state. As shown in Fig. 2C, the two distributions for the count rates of $|\uparrow\rangle$ and $|\downarrow\rangle$ are clearly resolved, and their medians match the high and low levels of the fluorescence trace in Fig. 2B. From the overlap between the two distributions, we obtain a projective readout fidelity of 91.9 ± 2.5% (*16*).

The long spin-orientation lifetime, extracted from Fig. 2B, implies that our ^{13}C nuclear spin is an exceptionally robust degree of freedom. To quantify the nuclear depolarization rate, the T_{1n} time was measured as a function of laser intensity. In the dark, no decay was observed on a time scale of 200 s (*15*). However, consistent with predictions from a spin-fluctuator model (*17, 18*), when illuminated with a weak optical field, T_{1n} dropped to 1.7 ± 0.5 s and increased linearly for higher laser intensities (Fig. 2D).

To probe the qubit's coherence time, our nuclear spin was again prepared via a projective measurement, after which an NMR Ramsey pulse sequence was applied. The final state of the nuclear spin was then detected via repetitive readout. The results (Fig. 3B) demonstrate that, in the dark, the nuclear coherence time T_{2n}^{*} is limited to about 8.2 ± 1.3 ms. The origin of this rel fast dephasing time can be understood by its direct correspondence with the populati time of the electronic spin $T_{1e} = 7.5 \pm$ (blue curve in Fig. 3B) (*19*). Because the el nuclear coupling $A_{\parallel}$ exceeds $1/T_{1e}$, a sing dom) flip of the electronic spin (from $|0\rangle$ is sufficient to dephase the nuclear spin.

To extend the nuclear memory time, w effectively decouple the electronic and spin during the storage interval. This is ac by subjecting the electronic spin to cor dissipation. Specifically, the NV center is by a focused green laser beam, resulting cal pumping of the NV center out of the m states ($|\pm 1\rangle$). In addition, the NV center a dergoes rapid ionization and deionization γ, proportional to the laser intensity (Fi When these transition rates exceed the hy coupling strength, the interaction between clear and electronic spins is strongly supp owing to a phenomenon analogous to m averaging (*17*).

Using this decoupling scheme, we sl Fig. 3C that the nuclear coherence time

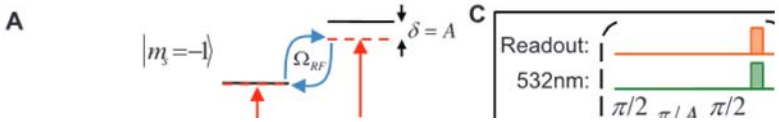

achieve single shot detection of the nuclear spin

enhanced by simply applying green laser light; in particular, 10 mW of green laser excitation yield an extended nuclear coherence time of $T_{2n}^{*} = 0.53 \pm 0.14$ s. This is an improvement of T_{2n}^{*} by almost two orders of magnitude as compared with measurements in the dark. The dependence of T_{2n}^{*} on green laser intensity shows a linear increase for low intensities and saturates around 1 s (Fig. 3E).

The observed limitation of coherence enhancement arises from dipole-dipole interactions of the nuclear qubit with other ^{13}C nuclei in the environment. In our sample, we estimate this average dipole-dipole interaction to be ~1 Hz, consistent with the limit in the observed coherence time. Further improvement of the nuclear coherence is achieved via a homonuclear rf decoupling sequence. The composite sequence (Fig. 3D) is designed to both average out the internuclear dipole-dipole interactions (to first order) and to compensate for magnetic field drifts. Applying this decoupling sequence in combination with green excitation can further extend the coherence time to beyond 1 s (Fig. 3E, blue points).

These measurements demonstrate that individual nuclear spins in isotopically pure diamond are exceptional candidates for long-lived memory qubits. The qubit memory performance was fully quantified by two additional measurements. First, the average fidelity was determined by preparing and measuring the qubit along three orthogonal directions. The average fidelity, $\overline{F} = 1/2(1 + \langle C \rangle)$, was extracted from the observed contrast (C) of the signal and is presented in Fig. 4A for two cases (with and without homonuclear decoupling) (*8*). Even for memory times up to 2.11 ± 0.3 s, the fidelity remained above the classical limit of $\frac{2}{3}$. Finally, a full characterization of our memory (at 1 s of storage time) was obtained via quantum process tomography. The corresponding χ matrix (Fig. 4C) reveals an average fidelity, $\overline{F} = 87 \pm 5\%$ (*15*).

To quantitatively understand the coherence extension under green illumination, we consider depolarization and dephasing of the nuclear spin due to optical illumination and interaction with the nuclear spin environment. Excitation with 532 nm ionizes, as well as deionizes, the NV center with a rate proportional to the laser intensity (*20*). Adding up the peak probabilities (Fig. 1C) for the nuclear rf transitions reveals a total transition probability of $63 \pm 5\%$. This is consistent with recent observations in which, under strong green illumination, the NV center is found to spend 30% of its time in an ionized state (*20*). In this state, rf-induced nuclear transitions are suppressed, because the depolarization rate of the electronic spin is much faster than the nuclear Rabi frequency (*20*). Because the hyperfine interaction is much smaller than the electronic Zeemann splitting, fl interactions between the electronic and ar spins can be neglected. However, presence of an off-axis dipolar hyperfin $A_{\perp}$, nuclear depolarization still occurs a $1/T_{1n} \sim \frac{A_{\perp}^2}{(\gamma_{13_C} B/2)^2 + \gamma^2} \gamma$ (*15*). Although th ple analysis is already in good agreement w observations (Fig. 2D), further insight is pr by a detailed 11-level model of NV dynami Because T_{1n} limits our readout, a careful ment of the external field (i.e., choosing A and enhanced collection efficiency should readout fidelities greater than 99%.

For ionization rates γ much larger th hyperfine interaction, the dephasing rate d on the parallel component of the dipol $1/T_{2n}^{*} = \Gamma_{opt} + \Gamma_{dd}$, where Γ_{dd} is the spin induced dephasing rate and $\Gamma_{opt} \sim \frac{A_{\parallel}^2}{\gamma}$ is t tically induced decoherence. The dash line in Fig. 3E demonstrates that this mod good agreement with our data. Applicatior decoupling sequence also allows us to su nuclear-nuclear dephasing. We find that th imperfection in this decoupling procedur nates from a finite rf detuning (*15*). Acc for this imperfection, we find excellent ment with our data, as shown by the dash line in Fig. 3E. Moreover, this model in that the coherence time increases almost l as a function of applied laser intensity, sug a large potential for improvement.

The use of even higher laser intens

Fig. 3. Nuclear spin coherence. **(A)** Model for repolarization and ionization dynamics. In the NV^- charge state, the electronic spin can be pumped via green illumination to $m_s = 0$ at a rate R. **(B)** Nuclear Ramsey experiment (red curve) depicting a dephasing time $T_{2n}^* = 8.2 \pm 1.3$ ms. The origin of this dephasing is the depolarization of the electronic spin (blue curve), with $T_{1e} = 7.5 \pm 0.8$ ms. **(C)** Nuclear Ramsey experiment

recent progress in the deterministic crea
arrays of NV centers (*26*) and NV-C pai
enables the exploration of scalable archit
(*28, 29*). Finally, recent experiments ha
demonstrated the entanglement of a phot
the electronic spin state of an NV cent
Combining the advantages of an ultralo
clear quantum memory with the possib
photonic entanglement opens up new ro
long-distance quantum communication an
state quantum repeaters (*1*).

References and Notes

1. L. M. Duan, C. Monroe, *Rev. Mod. Phys.* **82**, 120
2. T. D. Ladd *et al.*, *Nature* **464**, 45 (2010).
3. C. Langer *et al.*, *Phys. Rev. Lett.* **95**, 060502 (2
4. T. D. Ladd, D. Maryenko, Y. Yamamoto, E. Abe,
Phys. Rev. B **71**, 014401 (2005).
5. M. V. Balabas, T. Karaulanov, M. P. Ledbetter, D
Phys. Rev. Lett. **105**, 070801 (2010).
6. A. M. Tyryshkin *et al.*, *Nat. Mater.* **11**, 143 (20
7. A. Morello *et al.*, *Nature* **467**, 687 (2010).
8. M. V. Gurudev Dutt *et al.*, *Science* **316**, 1312 (
9. T. van der Sar *et al.*, http://arxiv.org/abs/arXiv:120
(2012).
10. P. Neumann *et al.*, *Science* **329**, 542 (2010).
11. G. de Lange, Z. H. Wang, D. Ristè, V. V. Dobro
R. Hanson, *Science* **330**, 60 (2010).
12. J. T. Barreiro *et al.*, *Nature* **470**, 486 (2011).
13. H. Krauter *et al.*, *Phys. Rev. Lett.* **107**, 080503 (2
14. G. Balasubramanian *et al.*, *Nat. Mater.* **8**, 383
15. Materials and methods are available as supplen
materials on *Science* Online.
16. A. H. Burrell, D. J. Szwer, S. C. Webster, D. M.
Phys. Rev. A **81**, 040302 (2010).
17. L. Jiang *et al.*, *Phys. Rev. Lett.* **100**, 073001 (2

with concurrent green illumination, showing $T_{2n} = 0.53 \pm 0.14$ s. (**D**) Experimental sequence used to measure the nuclear coherence time. A modified Mansfield-Rhim-Elleman-Vaughan (MREV) decoupling

18. L. Jiang *et al.*, *Science* **326**, 267 (2009).
19. P. Neumann *et al.*, *Science* **320**, 1326 (2008).

Room-Temperature Quantum Bit Memory Exceeding One Second

P. C. Maurer, G. Kucsko, C. Latta, L. Jiang, N. Y. Yao, S. D. Bennett, F. Pastawski, D. Hunger, N. Chisholm, M. Markham, D. J. Twitchen, J. I. Cirac and M. D. Lukin (June 7, 2012)

Science **336** (6086), 1283-1286. [doi: 10.1126/science.1220513]

Editor's Summary

Extending Quantum Memory

Practical applications in quantum communication and quantum computation require the building blocks––quantum bits and quantum memory––to be sufficiently robust and long-lived to allow for manipulation and storage (see the Perspective by **Boehme and McCarney**). **Steger *et al.*** (p. 1280) demonstrate that the nuclear spins of ^{31}P impurities in an almost isotopically pure sample of ^{28}Si can have a coherence time of as long as 192 seconds at a temperature of ~1.7 K. In diamond at room temperature, **Maurer *et al.*** (p. 1283) show that a spin-based qubit system comprised of an isotopic impurity (^{13}C) in the vicinity of a color defect (a nitrogen-vacancy center) could be manipulated to have a coherence time exceeding one second. Such lifetimes promise to make spin-based architectures feasible building blocks for quantum information science.